4-28-2014

Majorana Flat Bands in S -Wave Gapless Topological Superconductors

Shusa Deng
Dartmouth College

Gerardo Ortiz
University of Indiana

Amrit Poudel
Dartmouth College

Lorenza Viola
Dartmouth College

Majorana Flat Bands in s-Wave Gapless Topological Superconductors

Shusa Deng,[1] Gerardo Ortiz,[2] Amrit Poudel,[1] and Lorenza Viola[1]

[1]*Department of Physics and Astronomy, Dartmouth College, 6127 Wilder Laboratory, Hanover, NH 03755, USA*
[2]*Department of Physics, University of Indiana, Bloomington, Indiana 47405, USA*

(Dated: April 29, 2014)

We demonstrate how the non-trivial interplay between spin-orbit coupling and nodeless s-wave superconductivity can drive a *fully gapped* two-band topological insulator into a time-reversal invariant *gapless* topological superconductor supporting symmetry-protected Majorana flat bands. We characterize topological phase diagrams by a $\mathbb{Z}_2 \times \mathbb{Z}_2$ partial Berry-phase invariant, and show that, despite the trivial crystal geometry, no *unique* bulk-boundary correspondence exists. We trace this behavior to the *anisotropic* quasiparticle bulk gap closing, linear vs. quadratic, and argue that this provides a unifying principle for gapless topological superconductivity. Experimental implications for tunneling conductance measurements are addressed, relevant for lead chalcogenide materials.

PACS numbers: 73.20.At, 74.78.-w, 71.10.Pm, 03.67.Lx

The emergence of "topologically protected" Majorana edge modes is a hallmark of topological superconductors (TSs) [1]. Aside from their fundamental physical significance, Majorana modes are key building blocks in topological quantum computation [2], due to their potential to realize non-Abelian braiding. As a result, a wealth of different approaches are being pursued theoretically and experimentally in the quest for topological quantum matter [1], with recent highlights including broken time-reversal (TR) $p+ip$ superconductors, proximity-induced TR-invariant superconductivity in topological insulators (TIs), semiconductor-superconductor heterostructures, multiband superconductors and/or bilayer systems [3, 4], as well as experimental signatures of Majorana fermions in hybrid nanowires [5] and doped TIs [6]. Here, we propose a different paradigm, based on *topological gapless superconductivity in nodeless (s-wave) superconductors*.

Gapless superconductivity is a physical phenomenon where the quasiparticle energy gap is suppressed (that is, it vanishes at particular momenta), while the superconducting order parameter remains *finite*, strictly nonzero. This concept was anticipated on phenomenological grounds by Abrikosov and Gor'kov [7] in the context of TR pair-breaking effects in s-wave superconductors. Although certain unconventional superconductors may display similar behavior, their gapless nature results from the *nodal* character of the superconducting order parameter. In this work, the physical mechanism leading to a vanishing excitation gap is the spin-orbit coupling (SOC) in an otherwise *nodeless*, TR-invariant (centrosymmetric) multiband superconductor with bulk s-wave pairing.

A consequence of such a state of matter is the emergence of surface *Majorana flat bands* (MFBs) if the spatial dimension $D \geq 2$. It has been appreciated that protected zero-energy flat bands may exist in unconventional nodal superconductors – notably, at the surface of certain $d_{x^2-y^2}$-wave [8], d_{xy}-wave [9], and $d_{xy}+p$-wave superconductors [10]; superconductors with a mixture of d- and s-wave pairing [11]; $p\pm ip$ superconductors [12] and superconducting helical magnets with effective p-wave pairing [13] – as well as in the vortex core of topological defects [14]. Recently, a proposal for MFBs in nodeless s-wave (one-band) broken TR superconductors has also been put forward [15]. To the best of our knowledge, our model provides the first example of a TR-invariant s-wave gapless TS. We show that the *number* of Majorana edge modes in the non-trivial MFB phase (as opposed to just the *parity* of the number of Majorana pairs) is protected by a local chiral symmetry, a feature that is both crucial to understand robustness against perturbations and may be advantageous for topological quantum computation [16]. The dispersionless character of a MFB implies a large peak in the local density of states (LDOS) at the surface. Thus, while detecting Majorana fermions through a zero-bias conductance peak in scanning tunneling microscopy (STM) experiments is not viable in gapped $D \geq 2$ TSs, an unambiguous experimental signature is predicted in the gapless case [15, 17].

In addition to the above practical significance, an outstanding feature that our work unveils is the *anomalous, non-unique bulk-boundary correspondence* (BBC) that gapless TSs may exhibit: MFBs may emerge *only* along particular crystal directions, with *no* surface modes existing along others. While such an anomalous BBC is reminiscent of the directional behavior typical of topological crystalline phases [18], it does *not* stem simply from special crystal symmetries. Rather, the physical mechanism is rooted in the *anisotropic momentum dependence of the band degeneracy*: the quasiparticle gap may close non-linearly along certain directions, while it is linear (Dirac) along others. Only in the former case may a MFB exist at the corresponding edge. Accordingly, our findings suggest a *general* guiding principle for identifying and/or engineering materials supporting MFBs.

Model Hamiltonian.— We consider a two-band (say, orbitals c and d) TR-invariant s-wave superconductor on a 2D square lattice. By letting $\mathbf{k} \equiv (k_x, k_z)$ denote the wave-vector in the first Brillouin zone and

$\psi^\dagger_{\mathbf{k}} \equiv (c^\dagger_{\mathbf{k},\uparrow}, c^\dagger_{\mathbf{k},\downarrow}, d^\dagger_{\mathbf{k},\uparrow}, d^\dagger_{\mathbf{k},\downarrow}, c_{-\mathbf{k},\uparrow}, c_{-\mathbf{k},\downarrow}, d_{-\mathbf{k},\uparrow}, d_{-\mathbf{k},\downarrow})$, the relevant momentum-space Hamiltonian may be written as $H = \frac{1}{2}\sum_{\mathbf{k}} \left(\psi^\dagger_{\mathbf{k}} \hat{H}_{\mathbf{k}} \psi_{\mathbf{k}} - 4\mu\right)$, where the 8×8 matrix

$$\hat{H}_{\mathbf{k}} = s_z(m_{\mathbf{k}}\tau_z - \mu) + \tau_x(\lambda_{k_x}\sigma_x + \lambda_{k_z}\sigma_z) - \Delta s_x \tau_y \sigma_x. \quad (1)$$

Here, $s_\nu, \tau_\nu, \sigma_\nu$, $\nu = x, y, z$, are the Pauli matrices in the Nambu, orbital, and spin space, respectively, and tensor-product notation is understood. Physically, $m_{\mathbf{k}} \equiv u_{cd} - 2t(\cos k_x + \cos k_z)$, with u_{cd} and t representing the orbital-dependent on-site potential and the intraband hopping strength; μ is the chemical potential; $\lambda_{\mathbf{k}} \equiv (\lambda_{k_x}, \lambda_{k_z}) = -2\lambda(\sin k_x, \sin k_z)$ describes the interband SOC, and Δ is the mean-field gap, with the superconducting pairing term being an interband s-wave spin-triplet of the form $H_{\rm sw} = i\Delta\sum_j[(c^\dagger_{j,\uparrow}d^\dagger_{j,\downarrow} + c^\dagger_{j,\downarrow}d^\dagger_{j,\uparrow}) + \text{H.c.}]$, $\Delta \in$.

In addition to TR, particle-hole, and inversion symmetries [4], the Hamiltonian in Eq. (1) obeys a special (unitary) chiral symmetry, $[\hat{H}_{\mathbf{k}}, U_K]_+ = 0$, where $U_K \equiv s_x \otimes \tau_z \otimes I$ and I denotes the 2×2 identity matrix [19]. This symmetry will play an essential role in protecting MFBs. We may decouple $\hat{H}_{\mathbf{k}}$ into two 4×4 blocks by applying a suitable unitary transformation U, followed by a reordering P of the fermionic operator basis. Specifically, let $U \equiv \frac{1}{\sqrt{2}}\{[I\otimes(I + i\sigma_x)] \oplus [I\otimes(I - i\sigma_x)]\}$, with $P\psi^\dagger_{\mathbf{k}} \equiv (c^\dagger_{\mathbf{k},\uparrow}, d^\dagger_{\mathbf{k},\downarrow}, c_{-\mathbf{k},\downarrow}, d_{-\mathbf{k},\uparrow}, c^\dagger_{\mathbf{k},\downarrow}, d^\dagger_{\mathbf{k},\uparrow}, c_{-\mathbf{k},\uparrow}, d_{-\mathbf{k},\downarrow})$. Then H is transformed into $H' = \frac{1}{2}\sum_{\mathbf{k}}(\psi^\dagger_{\mathbf{k}}\hat{H}'_{\mathbf{k}}\psi_{\mathbf{k}} - 4\mu)$, with $\hat{H}'_{\mathbf{k}} = (PU)\hat{H}_{\mathbf{k}}(PU)^\dagger \equiv \hat{H}'_{1,\mathbf{k}} \oplus \hat{H}'_{2,\mathbf{k}}$. As in [4], $\hat{H}'_{1,\mathbf{k}}$ and $\hat{H}'_{2,\mathbf{k}}$ may be regarded as TR partners, and

$$\hat{H}'_{1,\mathbf{k}} = \begin{pmatrix} m_{\mathbf{k}}\sigma_z - \mu + \lambda_{\mathbf{k}}\cdot\vec{\sigma} & -i\Delta\sigma_y \\ i\Delta\sigma_y & -m_{\mathbf{k}}\sigma_z + \mu + \lambda_{\mathbf{k}}\cdot\vec{\sigma} \end{pmatrix},$$

with $\vec{\sigma} \equiv (\sigma_x, \sigma_y)$. The exact quasiparticle excitation spectrum obtained by diagonalizing $\hat{H}'_{1,\mathbf{k}}$ is given by:

$$\epsilon_{n,\mathbf{k}} = \pm\sqrt{m^2_{\mathbf{k}} + \Omega^2 + |\lambda_{\mathbf{k}}|^2 \pm 2\sqrt{\mu^2\lambda^2_{k_x} + \Omega^2(\lambda^2_{k_z} + m^2_{\mathbf{k}})}}, \quad (2)$$

where we assume the order $\epsilon_{1,\mathbf{k}} \le \epsilon_{2,\mathbf{k}} \le 0 \le \epsilon_{3,\mathbf{k}} \le \epsilon_{4,\mathbf{k}}$, and $\Omega^2 \equiv \mu^2 + \Delta^2$. If no SOC is present, $\lambda = 0$, then $\epsilon_{n,\mathbf{k}} = \pm(|m_{\mathbf{k}}| \pm |\Omega|)$, hence the gap closes ($\epsilon_{2,\mathbf{k}} = 0$) for $|m_{\mathbf{k}}| = |\Omega|$. By comparing $\epsilon_{2,\mathbf{k}}$ and $\epsilon_{3,\mathbf{k}}$, one can see that as long as $|u_{cd} \pm 4t| > |\Omega|$, there is a *continuous* region of gapless bulk modes, which corresponds to a gapless two-band superconductor with overlapping excitation spectrum [20]. If $\lambda \neq 0$, the situation is simplest at $\mu = 0$, in which case $\epsilon_{n,\mathbf{k}} = \pm\sqrt{\lambda^2_{k_x} + (\sqrt{m^2_{\mathbf{k}} + \lambda^2_{k_z}} \pm \Delta)^2}$, and $\epsilon_{2,\mathbf{k}} = 0$ when $\lambda_{k_x} = 0$, and $\lambda^2_{k_z} + m^2_{\mathbf{k}} = \Delta^2$. For instance, if $\lambda = t \neq 0$, this leads to $k_x \equiv k_{x,c} \in \{0, \pi\}$, and $k_z \equiv k_m = \pm\arccos\left(\frac{(u_{cd} - 2t\cos k_{x,c})^2 + 4t^2 - \Delta^2}{4t(u_{cd} - 2t\cos k_{x,c})}\right)$. Let $(k_x, k_z) \equiv (k_{x,c}, \pm k_m)$ denote the modes for which the bulk excitation spectrum closes. We then expect only a *finite* set of values k_m when $\lambda \neq 0$ for arbitrary μ. The quantum critical lines are determined by $\Delta = \pm m_{\mathbf{k}_c}$, with $\mathbf{k}_c \equiv (k_{x,c}, k_{z,c})$ and $k_{z,c} \in \{0, \pi\}$) [Fig. 1(a)].

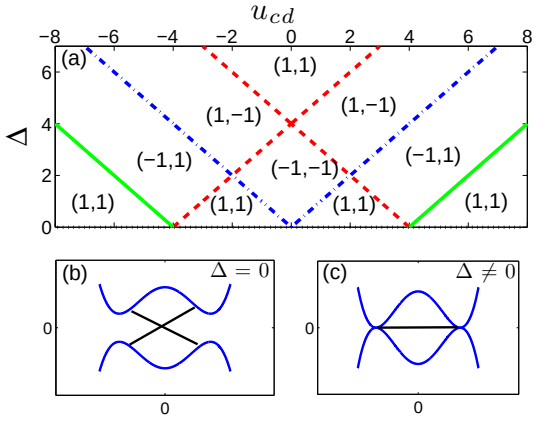

FIG. 1: (Color online) Panel (a): Phase diagram of H [Eq. (1)] for $\mu = 0 = \lambda = 1$. Each phase is labelled by the partial Berry-phase parities $(P_{B,0}, P_{B,\pi})$. The topological numbers do not change under $\Delta \mapsto -\Delta$. Panels (b) and (c): Sketch of the spectrum of H with $\Delta = 0$ in a TI phase, and with $\Delta \neq 0$ in a TS flat-band phase, respectively.

In the limit $\Delta = 0$, our Hamiltonian reduces (up to unitary equivalence) to a TI model [21]. A qualitative comparison of the spectrum with open boundary conditions (OBC) along $\hat{z}$ with $\Delta = 0$ vs. $\Delta \neq 0$ is shown in Fig. 1(b)-(c). Remarkably, we may consider our gapless TS to arise from doping a TI with *fully-gapped*, nodeless (spin-triplet) s-wave superconductivity. More intuitively, an alternative route to realize our gapless TS is by turning on a suitable SOC in a two-band *gapless* superconductor, as the effect of $\lambda \neq 0$ is to separate the overlapping excitation spectrum and only leave a vanishing gap at a finite number of points. Thus, our nontrivial quasiparticle spectrum is a combined effect of SOC and superconducting order parameter. The most striking aspect of such a spectrum is the fact that *the quasiparticle gap closing is anisotropic*: the gap vanishes *linearly* along k_x [i.e., $\sim (k_x - k_{x,c})$] and *quadratically* along k_z [i.e., $\sim (k_z - k_m)^2$]. As we shall soon see, this peculiar behavior will manifest directly into an anomalous BBC.

Topological response.— As a result of the gapless nature of the bulk excitation spectrum, topological invariants (such as the partial Chern number [4]) applicable to 2D TR-invariant gapped TS systems are no longer appropriate. This motivates the use of *partial* Berry-phase indicators [4]. In particular, we study the partial Berry phase of the two occupied negative bands of one Kramers' sector only, $\hat{H}_{1,\mathbf{k}}$, for each k_z (or k_x), namely, $B_{n,k_z}, n = 1, 2$, since the Berry phase of all the negative bands of $\hat{H}_{1,\mathbf{k}}$ and $\hat{H}_{2,\mathbf{k}}$ is always trivial [4]. We can then compute the partial Berry phase parity for each k_z as

$$P_{B,k_z} = (-1)^{\text{mod}_{2\pi}(B_{+,k_z})/\pi},\ B_{+,k_z} \equiv B_{1,k_z} + B_{2,k_z}, \quad (3)$$

and define a $\mathbb{Z}_2$ topological number as $\prod_{k_z} P_{B,k_z}$. How-

ever, similar to the gapped case [4], the latter fails to identify quantum-critical lines between phases that share the same $\mathbb{Z}_2$ number. For the purpose of identifying all the phase transitions and characterizing the *whole* phase diagram in Fig. 1(a), a $\mathbb{Z}_2 \times \mathbb{Z}_2$ indicator is necessary. Specifically, we define our topological invariant as $(P_{B,k_z=0}, P_{B,k_z=\pi})$ [marked in each phase on Fig. 1(a)], which correctly signals a phase transition whenever a jump of either $P_{B,k_z=0}$ or $P_{B,k_z=\pi}$ occurs. Since, as expected for a consistent bulk behavior, it turns out that $(P_{B,k_x=0}, P_{B,k_x=\pi}) = (P_{B,k_z=0}, P_{B,k_z=\pi})$, we shall just write the $\mathbb{Z}_2 \times \mathbb{Z}_2$ invariant as $(P_{B,0}, P_{B,\pi})$ henceforth. Note that while ultimately such a $\mathbb{Z}_2 \times \mathbb{Z}_2$ invariant involves only the partial Berry phase at $\mathbf{k} = \mathbf{k_c}$, the reason for the more general definition of the topological numbers at $k_z \neq k_{z,c}$ is related to the BBC, as we discuss next.

Bulk-boundary correspondence.— In a gapped TR-invariant TS, the BBC defines the relation between bulk topological invariants and the (parity of the) number of TR pairs of edge states [1, 4, 22]. To understand the BBC in our gapless model, we contrast two situations: BC1—periodic boundary conditions (PBC) along $\hat{z}$, and OBC along $\hat{x}$; BC2— PBC along $\hat{x}$, and OBC along $\hat{z}$. Fig. 2 shows how the excitation spectrum changes as a function of Δ for BC1 (top panels) and BC2 (bottom panels) for representative parameter choices in phases labelled by $(P_{B,0}, P_{B,\pi}) = (1,1)$ [panels (a) and (c)], and $(P_{B,0}, P_{B,\pi}) = (1,-1)$ [panels (b) and (d)]. In (a) there are two pairs of Majorana modes on each boundary for $k_z = 0$, but no Majorana edge modes in (c); likewise, in (b) there is a MFB for $k_m < |k_z| \leq \pi$ ($k_m \approx 1.8$), but again no Majorana edge modes in (d). As further investigation under BC1 reveals, when $P_{B,k_z} = -1$ a *single* TR-pair of Majorana *edge* modes exists for that k_z-value on each boundary. Thus, a MFB is generated when there is a dense set of k_z for which $P_{B,k_z} = -1$. On the contrary, the partial Berry phase for $k_x \neq k_{x,c}$ is always trivial (i.e., $P_{B,k_x} = 1$); and when $P_{B,k_{x,c}} = -1$, it corresponds to gapless *bulk* modes for that $k_{x,c}$.

The above results demonstrate the asymmetry between the $\hat{x}$ and $\hat{z}$ directions notwithstanding their geometrical equivalence – in direct correspondence with the anisotropic momentum dependence of the bulk excitation gap, as anticipated [23]. We stress that although the choice of Hamiltonian in Eq. (1) is motivated by our earlier work [4], different physical realizations of s-wave gapless TR-invariant TSs may be envisioned as long as a similar mechanism is in place: notably, we may change $H_{\rm sw}$ to *interband s-wave spin-singlet*, $H'_{\rm sw} = \sum_j \Delta[(c^\dagger_{j,\uparrow} d^\dagger_{j,\downarrow} - c^\dagger_{j,\downarrow} d^\dagger_{j,\uparrow}) + \text{H.c.}]$, while also ensuring that the strength of the SOC is sufficiently anisotropic, e.g., $(\lambda_{k_x}, \lambda_{k_z}) = -2(\lambda_x \sin k_x, \lambda_z \sin k_z)$, with $\lambda_z \ll \lambda_x$. Based on these observations, we conjecture that the momentum asymmetry of the (bulk) excitation gap closing is a necessary condition for anomalous BBC, and that MFBs are necessarily associated with higher-than-linear closing. Direct calculation confirms that this conjecture holds across a variety of models supporting surface flat bands: in particular, anomalous BBC is observed in spin-triplet $p_x + ip_y$ TSs [12], in both s-wave and $d_{x^2-y^2}$-wave spin-singlet TSs [15], as well as a TR-broken TI model [24]. Interestingly, MFBs emerge along *both* spatial directions in d_{xy} TSs [9], consistent with the symmetric (quadratic) closing of the bulk gap.

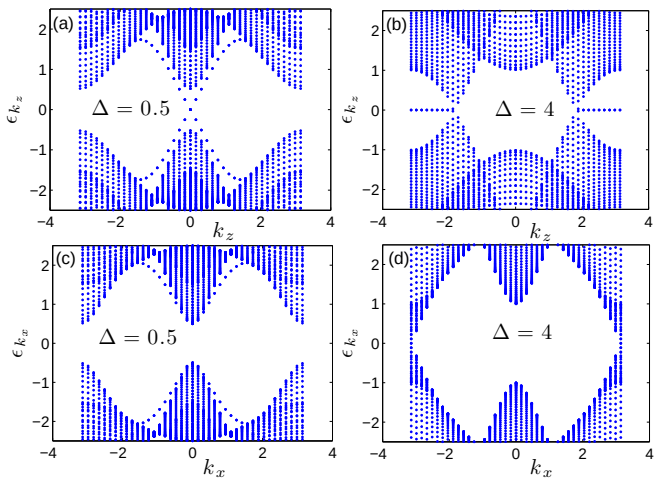

FIG. 2: (Color online) Excitation spectrum of H [Eq. (1)] for $\mu = 0, t = \lambda = u_{cd} = 1$. Top (bottom) panels correspond to BC1 (BC2), whereas right vs. left columns correspond to $(P_{B,0}, P_{B,\pi}) = (1,1)$ vs. $(1,-1)$. System size: $N_x = N_z = 40$.

Observable signatures of Majorana flat band.— The tunneling current between a STM and the material is proportional to the surface LDOS of electrons [25]. Results of LDOS calculations are shown in Fig. 3, together with the corresponding bulk density of states (DOS): a huge (small) peak for the LDOS (DOS) is seen at zero energy under BC1 in (a), whereas no zero-energy peak occurs under BC2 in (b). While the quantitative difference between the LDOS vs. DOS peaks in panel (a) does indicates that the zero-energy modes are located on the boundary, the qualitative difference between panels (a) and (b) reinforces the asymmetric behavior under the two boundary conditions shown in Fig. 2. It is instructive to compare to a typical gapped TS, e.g., the TR-invariant model discussed in Ref. [4]. Although in this case Majorana edge modes exist in a nontrivial phase regardless of the direction along which OBC are assigned, *no* peak in LDOS (DOS) is seen at zero energy for $D > 1$ [panels (c)-(d)]: in 2D (and 3D), the contribution to the LDOS from the finite number of Majorana edge modes is washed out by the extensive one from the bulk modes as the system size grows. Thus, a mechanism other than the existence of a finite number of Majoranas is needed to explain a zero-bias peak in 2D (3D) fully-gapped superconductors.

Robustness of Majorana flat band.— Let us first consider a TR-preserving perturbation of the form $H_p = \sum_{j_x,k_z,k'_z,\sigma} u_p \, (c^\dagger_{j_x,k_z,\sigma} c_{j_x,k'_z,\sigma} + d^\dagger_{j_x,k_z,\sigma} d_{j_x,k'_z,\sigma}) + \text{H.c.}$,

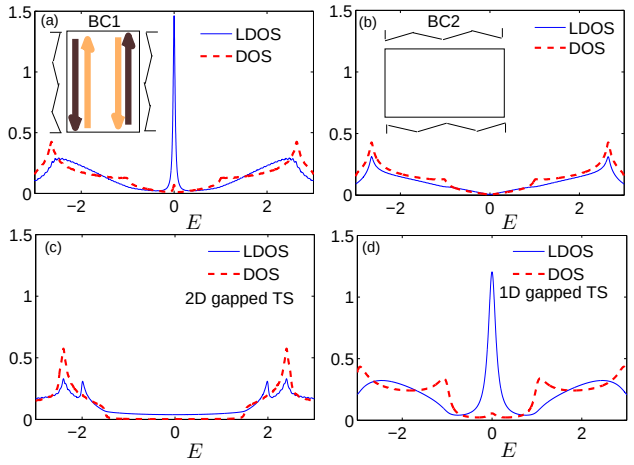

FIG. 3: (Color online) Panels (a) and (b): LDOS and DOS for H [Eq. (1)] for $\mu = 0, t = \lambda = u_{cd} = 1, \Delta = 4$. Insets: The jagged lines signify cuts of the system, implying that in BC1 (BC2) the OBC is along the $\hat{x}$ ($\hat{z}$). In (a), the brown (orange) arrows indicate a continuum of TR-pairs of Majoranas on each boundary, propagating along opposite directions. Panels (c) and (d): LDOS and DOS for a gapped TS in 2D and 1D. System size: $(N_x, N_z) = (80, 400)$ (a), $(N_x, N_z) = (400, 80)$ (b), $(N_x, N_z) = (80, 400)$ (c), $N_x = 80$ (d).

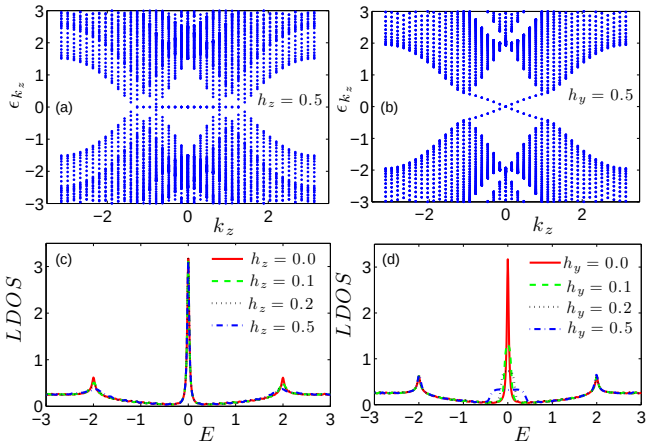

FIG. 4: (Color online) Excitation spectrum of $H + H_\nu$ for $\mu = 0, t = \lambda = 1, u_{cd} = 4, \Delta = 2$. Panels (a) and (b): in-plane vs. out-of-plane field. Panels (c) and (d): LDOS for increasing field strength along $\hat{z}$ vs. $\hat{y}$. System size: $(N_x, N_z) = (40, 40)$ [(a), (b)], $(N_x, N_z) = (40, 400)$ [(c), (d)].

where $k'_z \in \{-k_z, \pi - k_z\}$, $u_p \in$. Since H_p allows Majorana modes at k_z and k'_z to couple with each other, it could significantly change the number of edge modes in principle. However, the zero-energy modes on the left (right) boundary of $\hat{H}'_{1,k_z}$, say $\gamma_{k_z,\ell}$ ($\ell = L, R$), may be taken to be eigenstates of $\mathcal{K}$, i.e., $\mathcal{K}\gamma_{k_z,\ell} = \pm\gamma_{k_z,\ell}$, when there is only one edge mode on each boundary for k_z. Thus, when there is *only one pair of zero-energy modes in the bulk*, at $k_z = \pm k_m$, all the zero-energy edge modes on the same boundary can be continuously deformed one into another, which guarantees that they belong to the same sector of $\mathcal{K}$. Therefore, any local perturbation that preserves both chirality and TR cannot lift the degeneracy of the zero-energy modes belonging to the same sector of $\mathcal{K}$, leaving the MFB stable. However, *the protection from $\mathcal{K}$ may fail when there is an even number of pairs of zero-energy bulk modes*: e.g., in the phase $(P_{B,0}, P_{B,\pi}) = (-1, -1)$, the MFB is not robust against H_p, since now Majoranas on the same boundary may belong to different sectors of $\mathcal{K}$. Thus, not only does the *parity* of the number of Kramers' pairs of Majoranas still play an important role, but also the *number* of edge modes in the MFB is conserved as long as both symmetries are respected and there is only one pair of bulk gapless modes. Similarly, the MFB is robust against another natural TR-preserving perturbation, namely, *intraband* s-wave pairing, $H_s = \Delta_c \sum_j (c^\dagger_{j,\uparrow} c^\dagger_{j,\downarrow} + \Delta_d \sum_j d^\dagger_{j,\uparrow} d^\dagger_{j,\downarrow}) + \text{H.c.}$, $\Delta_c, \Delta_d \in$, which anti-commutes with U_K.

Next, consider TR-breaking perturbations due to a static magnetic field [4, 26], $H_\nu = h_\nu \sum_j \psi^\dagger_j \sigma_\nu \psi_j$, where $\nu = \hat{x}, \hat{z}$ ($\hat{y}$) correspond to in-plane (out-of-plane) directions. The response to an in-plane field is similar in both directions, with the MFB remaining flat, Fig. 4(a). Under a magnetic field h_y, instead, the MFB becomes unstable, Fig. 4(b). The effect of the magnetic field along different directions may be understood through its relation with chirality. Specifically, the $\hat{x}$ and $\hat{z}$-components of H_ν anti-commute with $\mathcal{K}$, whereas H_y *commutes* with $\mathcal{K}$. Accordingly, chirality-protection is lost in this case. The LDOS in the presence of Zeeman fields along in-plane ($\hat{z}$) and out-of-plane ($\hat{y}$) directions is shown in Fig. 4 (c)-(d): the peak at zero energy stays almost unchanged as h_z increases, whereas it is strongly suppressed when $h_y \neq 0$. This is consistent with the results from the excitation spectrum shown above. Moreover, the behavior of the LDOS under a magnetic field along an *arbitrary* direction on the $\hat{x}$-$\hat{z}$ plane is similar to the one under h_z. We may then infer that a MFB responds to a uniform Zeeman field along a certain direction in a similar way as to a magnetic impurity field along the same direction. Thus, the MFB will be robust in the presence of in-plane magnetic impurities, which may be unavoidable in real materials. Lastly, we investigated the effect of on-site disorder along the boundary, $H_d = \sum_j v_j (c^\dagger_{j,\uparrow} c_{j,\uparrow} + c^\dagger_{j,\downarrow} c_{j,\downarrow} + d^\dagger_{j,\uparrow} d_{j,\uparrow} + d^\dagger_{j,\downarrow} d_{j,\downarrow}) + \text{H.c}$, where $v_j \in$ is a Gaussian random potential. The MFBs is robust against weak disorder so long as chirality is preserved, with the zero-energy peak in the LDOS remaining qualitatively intact.

Conclusion.— Majorana modes in gapless TSs can manifest themselves through new signatures, such as the emergence of a chirality-protected MFB which may depend crucially on the nature of the boundary. Such an anomalous, non-unique, BBC in 2D (3D) gapless TSs allows for a more unambiguous signature in tunneling experiments than gapped TSs may afford. The anisotropic, linear vs. non-linear, vanishing of the quasiparticle bulk

excitation gap at particular momenta is the unifying principle behind such anomaly. Our model provides an explicit realization of a TR-invariant two-band gapless TS, where an anisotropic excitation spectrum arises from the interplay of conventional s-wave superconductivity with a SOC whose form is motivated by band-structure studies in $Pb_xSn_{1-x}Te$ [27]. Thus, we expect that materials in this class may be natural candidates for the experimental search of TR-invariant gapped [4] or gapless TSs.

We thank Jake Taylor and Yuji Matsuda for discussions. Support from the NSF through grants No. PHY-0903727 and PHY-1104403 (to LV) is acknowledged.

[1] B. A. Bernevig and T. L. Hughes, *Topological Insulators and Topological Superconductors* (Princeton University Press, 2013).

[2] A. Y. Kitaev, Ann. Phys. **321**, 2 (2003); C. Nayak, S. H. Simon, A. Stern, M. Freedman, and S. D. Sarma, Rev. Mod. Phys. **80**, 1083 (2008).

[3] G. Moore and N. Read, Nucl. Phys. B **360**, 362 (1991); L. Fu and C. L. Kane, Phys. Rev. Lett. **100**, 096407 (2008); J. Linder, Y. Tanaka, T. Yokoyama, A. Sudbo, and N. Nagaosa, Phys. Rev. Lett. **104**, 067001 (2010); R. M. Lutchyn, J. D. Sau, and S. D. Sarma, Phys. Rev. Lett. **105**, 077001 (2010); B. Seradjeh, Phys. Rev. B **86**, 121101(R) (2012).

[4] S. Deng, L. Viola, and G. Ortiz, Phys. Rev. Lett. **108**, 036803 (2012); S. Deng, G. Ortiz, and L. Viola, Phys. Rev. B **87**, 205414 (2013).

[5] V. Mourik, K. Zuo, S. M. Frolov, S. R. Plissard, E. P. A. M. Bakkers, and L. P. Kouwenhoven, Science **25**, 1003 (2012); A. Das, Y. Ronen, Y. Most, Y. Oreg, M. Heiblum, and H. Shtrikman, Nature Phys. **8**, 887 (2012); L. P. Rokhinson, X. Liu, and J. K. Furdyna, Nature Phys. **8**, 795 (2012); M. T. Deng, C. L. Yu, G. Y. Huang, M. Larsson, P. Caroff, and H. Q. Xu, Nano Lett. **12**, 6414 (2012).

[6] S. Sasaki, Z. Ren, A. A. Taskin, K. Segawa, L. Fu, and Y. Ando, Phys. Rev. Lett. **107**, 217001 (2011); G. Balakrishnan, L. Bawden, S. Cavendish, and M. R. Lees, Phys. Rev. B **87**, 140507(R) (2013); M. Novak, S. Sasaki, M. Kriener, K. Segawa, and. Y. Ando, **88**, 140502(R) (2013).

[7] A. A. Abrikosov and L. P. Gor'kov, JETP **12**, 1243 (1961).

[8] C. Hu, Phys. Rev. Lett. **72**, 1526 (1994).

[9] M. Sato and S. Fujimoto, Phys. Rev. Lett. **105**, 217001 (2010); M. Sato, Y. Tanaka, K. Yada, and T. Yokoyama, Phys. Rev. B **83**, 224511 (2011).

[10] Y. Tanaka, Y. Mizuno, T. Yokoyama, K. Yada, and M. Sato, Phys. Rev. Lett. **105**, 097002 (2010).

[11] A. P. Schnyder and S. Ryu, Phys. Rev. B **84**, 060504(R) (2011).

[12] C. L. M. Wong, J. Liu, K. T. Law and P. A. Lee, Phys. Rev. B **88**, 060504(R) (2013).

[13] I. Martin and A. F. Morpurgo, Phys. Rev. B **85**, 144505 (2012).

[14] G. E. Volovik, JETP Lett. **93**, 66 (2011).

[15] J. You, C. H. Oh, and V. Vedral, Phys. Rev. B **87**, 054501 (2013); J. You, A. H. Chan, C. H. Oh, and Vlatko Vedral, arXiv:1306.2436.

[16] J. Alicea, Y. Oreg, G. Refael, F. Oppen, and M. P. A. Fisher, Nature Phys. **7**, 412 (2011); A. R. Akhmerov, Phys. Rev. B **82**, 020509(R) (2010).

[17] J. Liu, A. C. Potter, K.T. Law, and P. A. Lee, Phys. Rev. Lett. **109**, 267002 (2012); D. Bagrets and A. Altland, Phys. Rev. Lett. **109**, 227005 (2012).

[18] L. Fu, Phys. Rev. Lett. **106**, 106802 (2011); C. Y. Teo, and T. L. Hughes, Phys. Rev. Lett. **111**, 047006 (2013).

[19] Using U_K to define a chiral symmetry operator $\mathcal{K}$ by its action on the Nambu basis vector, i.e. $\mathcal{K}\,(\psi_{\mathbf{k}})_j\,\mathcal{K}^{-1} \equiv \sum_l (U_K)_{jl}\,(\psi_{\mathbf{k}})_l$, we obtain the following fermionic transformation properties: $\mathcal{K}\,c(d)_{\mathbf{k},\uparrow}\mathcal{K}^{-1} = c^\dagger(-d^\dagger)_{-\mathbf{k},\uparrow}$, $\mathcal{K}\,c^\dagger(d^\dagger)_{\mathbf{k},\uparrow}\mathcal{K}^{-1} = c(-d)_{-\mathbf{k},\uparrow}$, and $\mathcal{K}\,c(d)_{\mathbf{k},\downarrow}\mathcal{K}^{-1} = c^\dagger(-d^\dagger)_{-\mathbf{k},\downarrow}$, $\mathcal{K}\,c^\dagger(d^\dagger)_{\mathbf{k},\downarrow}\mathcal{K}^{-1} = c(-d)_{-\mathbf{k},\downarrow}$.

[20] D. Mandrus, J. Hartge, C. Kendziora, L. Mihaly, and L. Forro, Europhys. Lett. **22**, 199 (1993); G. Seyfarth, J. P. Brison, M.-A. Masson, J. Flouquet, K. Izawa, Y. Matsuda, H. Sugawara, and H. Sato, Phys. Rev. Lett. **95**, 107004 (2005); M. A. Tanatar, J. Paglione, S. Nakatsuji, D. G. Hawthorn, E. Boaknin, R. W. Hill, F. Ronning, M. Sutherland, L. Taillefer, C. Petrovic, P. C. Canfield, and Z. Fisk, Phys. Rev. Lett. **95**, 067002 (2005).

[21] G. Rosenberg and M. Franz, Phys. Rev. B **82**, 035105 (2010).

[22] L. Isaev, Y. H. Moon, and G. Ortiz, Phys. Rev. B **84**, 075444 (2011).

[23] Interestingly, $\prod_{k_z} P_{B,k_z} = \prod_{k_x} P_{B,k_x}$, which indicates consistent bulk properties as a whole, although the topological numbers for each k_x, k_z may differ individually.

[24] T. Paananen and T. Dahm, Phys. Rev. B **87**, 195447 (2013).

[25] T. D. Stanescu, S. Tewari, J. D. Sau, and S. D. Sarma, Phys. Rev. Lett. **109**, 266402 (2012); S. Matsuura, P.-Y. Chang, A. P. Schnyder, and S. Ryu, New J. Phys. **15**, 065001 (2013).

[26] E. Dumitrescu, J. D. Sau, and S. Tewari, arXiv: 1310.7938.

[27] J. O. Dimmock, I. Melngailis, and A. J. Strauss, Phys. Rev. Lett. **16**, 1193 (1966).